Journal of Structural Geology 33 (2011) 32–37

Contents lists available at ScienceDirect

Journal of Structural Geology

journal homepage: www.elsevier.com/locate/jsg

Sheets within diapirs – Results of a centrifuge experiment

C. Dietl [a,*], Hemin Koyi [b]

[a] Institut für Geowissenschaften, Goethe-Universität, Altenhöferallee 1, 60438 Frankfurt, Germany
[b] Geocentrum, Uppsala Universitet, Villavägen 16, Uppsala, Sweden

ARTICLE INFO

Article history:
Received 21 February 2010
Received in revised form
9 September 2010
Accepted 30 October 2010
Available online 10 November 2010

Keywords:
Centrifuge
Diapir
Balloon-on-string
Finger-shaped
Composite

ABSTRACT

We carried out a centrifuge experiment to model the diapiric rise of a stratified PDMS layer from three perturbations through a non-Newtonian, ductile overburden. The experiment carried out at 700 *g* resulted in three composite diapirs fed by different PDMS layers. The three resulting diapirs represent two different stages of diapirism. One of the diapirs (diapir 1), which reached its level of neutral buoyancy and extruded at the surface of the model, was tabular in profile and copied by an internal intrusive body. The other two diapirs (diapirs 2 and 3) were still in the ascending stage when centrifuging was stopped and thus did not extrude at the surface. They displayed a typical balloon-on-string geometry, which develops at a high viscosity contrast between a highly viscous overburden and a less viscous buoyant material. The internal geometry of these last two diapirs, fed by the lower impure PDMS, however, did not copy the shape of their precursors. Instead, they had a finger-like shape. The finger geometry of the internal part of the diapirs might be the result of the higher viscosity of the impure lower PDMS intruding a less viscous clean PDMS. Compared to nature, diapir 1 represents a fully developed concentrically expanded pluton or nested diapir, while diapirs 2 and 3 resemble composite plutons which host magma batches of dyke-like geometry. Based on the results of our experiment we suggest that truly concentrically expanded plutons develop from the latter.

1. Introduction

Numerous plutons contain sheet-like (mafic) dikes and swarms of (mafic) enclaves (Fig. 1a and b); the latter are commonly regarded as disintegrated dikes (Sparks and Marshall, 1986; Frost and Mahood, 1987). Examples include the Chila Pluton in Ethiopia (Tadesse-Alemu, 1998; Jungmann, 2009; Fig. 2a) and the Cannibal Creek Pluton in Australia (Paterson and Vernon, 1995; Fig. 2b). Most of these dikes are not dikes sensu strictu, because they do not crack solid rock which reacts elastically on the high magma pressure at the tip of the dike (Lister and Kerr, 1991). Rather they propagate "ductilely" through a mainly viscously behaving magma. It is this propagation process which finally leads to disintegration of these contigous bodies and to the formation of enclave swarms. Nevertheless, they are dikes in a geometric sense, i.e. they have a high length/width ratio (Spera, 1980), and are probably driven – as dikes s.s. – by a combination of buoyancy and the magma pressure within the dike (Petford et al., 2000).

Other plutons consist of several magma batches which are nested into each other in a concentric manner. Two of the most intriguing examples of these composite plutons are the Joshua Flat-Beer Creek Pluton in California (Dietl and Longo, 2007; Fig. 3a) and the Ardara Pluton in Ireland (e.g. Paterson and Vernon, 1995; Sigesmund and Becker, 2000; Fig. 3b). Both features may be related to each other: the dikes could be the feeders of the magma batches which form the composite plutons. However, this possible genetic relation is neither proven, nor it is known yet *how* they are related to each other. We carried out a centrifuge model which provides some interesting answers to these questions.

2. The experiment

The model consisted of a 34 mm thick non-Newtonian, ductile overburden with a density ρ of 1.55 g/cm^3 and a viscosity μ of 2×10^6 Pa s at a strain rate of 2.5×10^{-3} s^{-1} and a buoyant, Newtonian polydimethylsiloxane (PDMS) (Weijermars, 1986; Koyi, 1991) layer of 6 mm thickness that was placed beneath the overburden. Both, the overburden and the buoyant layer were stratified in order to visualize the deformation structures within them. Stratification in the overburden was passive. The passive layers in the overburden were coloured brown (7 strata, each 4 mm thick) and dark-grey (6 strata, each 1 mm thick), respectively. However, the buoyant layer consisted of two mechanically active layers; an upper clean PDMS

* Corresponding author.
E-mail address: c.dietl@em.uni-frankfurt.de (C. Dietl).

0191-8141/$ – see front matter © 2010 Elsevier Ltd. All rights reserved.
doi:10.1016/j.jsg.2010.10.010

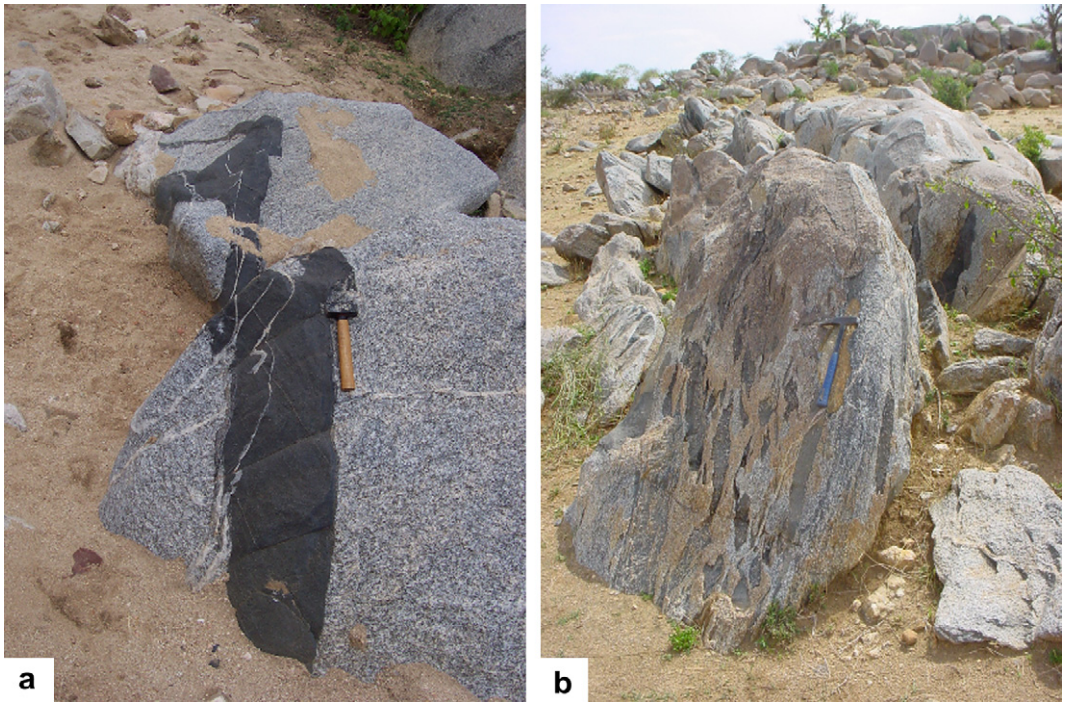

Fig. 1. a) Mafic dike within the Chila Pluton (Ethiopia). b) Swarm of mafic enclaves within the Joshua Flat-Beer Creek Pluton (California).

layer (4 mm thick, $\rho = 0.964$ g/cm^3, $\mu = 2.4 \times 10^4$ Pa s) which was stained purple and a lower impure light-grey layer (2 mm thick, $\rho = 1.17$ g/cm^3, $\mu = 5 \times 10^5$ Pa s) which consisted of sand-contaminated PDMS. The model was topped by two thin plasticine strata, each 1 mm thick; the lower one was light-grey, the upper one white with a strain grid on its surface. To initiate three diapirs in the model, three perturbations of purple PDMS were initially put on top of the buoyant PDMS layer (Fig. 4). The ductile overburden simulated lower-crustal, siliciclastic rocks ($\rho \sim 2.7$ g/cm^3, $\mu \sim 10^{22}$ Pa s), the pure PDMS represented a felsic and highly viscous magma or partially molten silicic rock with $\rho \sim 1.7$ g/cm^3 and $\mu \sim 10^{20}$ Pa s and the impure PDMS stands for a mafic magma with $\rho \sim 2$ g/cm^3 and $\mu \sim 10^{21}$ Pa s. Viscosities of the "model magmas" are, of course, too high and the density too low with respect to a natural system. However, the observations from the model that we describe below and our interpretations are probably also valid for less viscous natural systems which were not possible to model with the currently available analogue materials.

The setup of the model is displayed in Fig. 4, the material properties and scaling factors are listed in Table 1.

The experiment was centrifuged for 6 min and 30 s at 700 *g* and stopped when the first PDMS diapir reached the model surface. The model was photographed in top view and sectioned for further examination.

During centrifuging, three diapirs were initiated from the three perturbations. One of them (diapir 1) had pierced through the overburden and both the plasticine strata and spread on top of the model (Fig. 5a) to form an asymmetric, tabular extrusion (Fig. 5b).

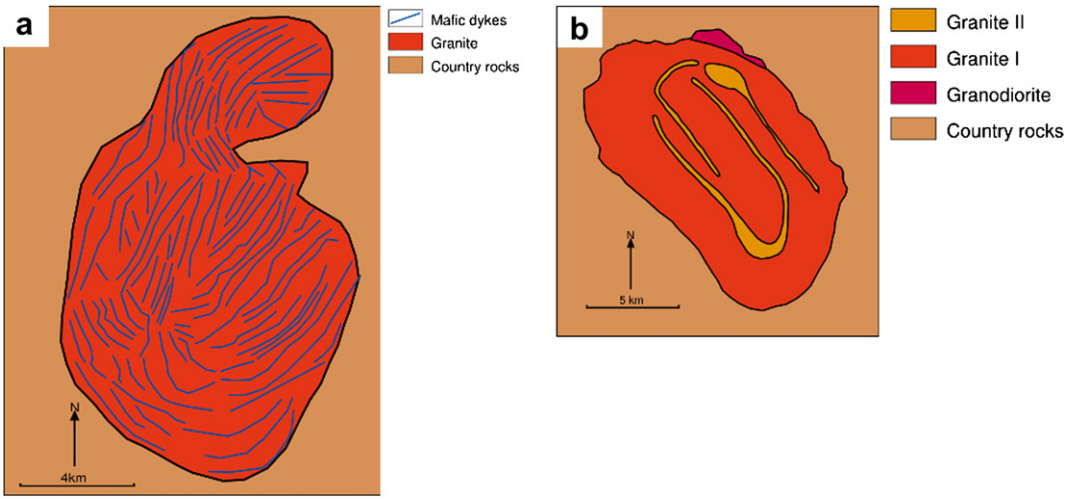

Fig. 2. a) Geolgical map of the Chila Pluton (Jungmann, 2009). b) Geological map of the Cannibal Creek Pluton (redrawn from Paterson and Vernon, 1995). Both these plutons are characterised by numerous dikes which crosscut the pluton in a regular, concentrical pattern.

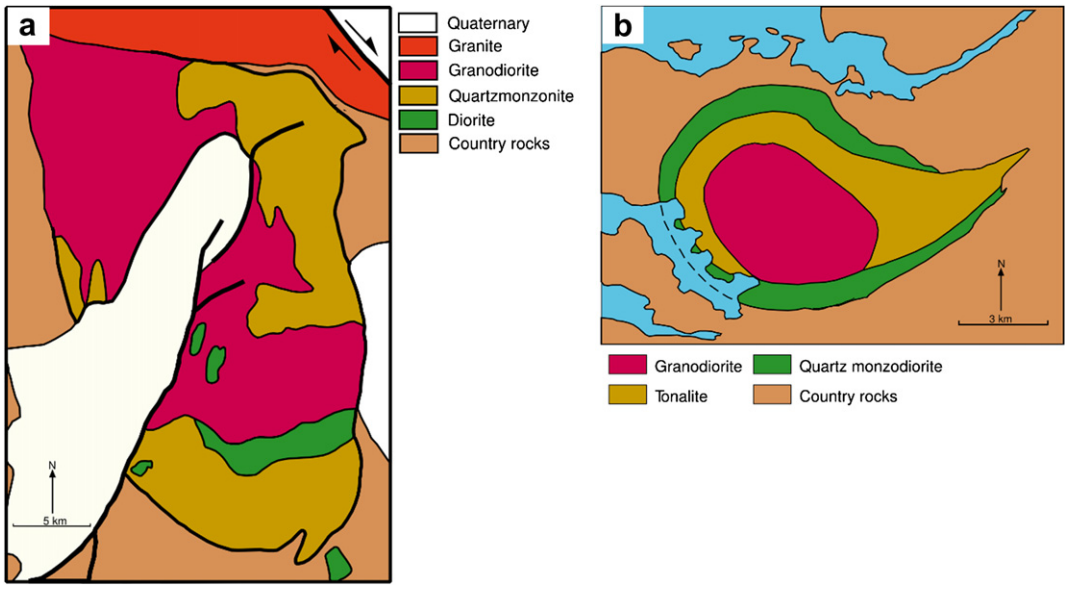

Fig. 3. a) Geological map of the Joshua Flat-Beer Creek Pluton (redrawn from Dietl and Longo, 2007). b) Geological map of the Ardara Pluton (redrawn from Paterson and Vernon, 1995). These are typical composite plutons consisting of several magma batches which are described in literature as concentrically expanded plutons or nested diapirs.

Around diapir 1, a fully developed rim syncline had formed. Even the two plasticine layers on top of the model were incorporated into the rim syncline and were deformed into recumbent, isoclinal folds. Where deformation is strongest – due to the extrusion of the PDMS – the upper, overturned limb of these folds is pulled off and thrusts have formed along which the tabular diapir head moved sideways during its extrusion (Fig. 5b). Diapir 1 is a composite structure and consists of both buoyant strata (i.e. the clean and the impure PDMS materials). The grey, impure PDMS copies the external geometry of the diapir which is formed by the purple PDMS (Fig. 5b) and which is almost elliptical in map view and tabular in profile. Hereby, diapir 1 resembles geometrically a typical composite pluton.

Diapirs 2 and 3 had reached the upper half of the overburden when centrifuging was stopped. Nevertheless, they caused doming of their overburden and brittle fracturing of the plasticine strata. Both these diapirs have "balloon-on-string" geometry (Jackson and Talbot, 1989) with relatively thin stem in relation to the diapir head

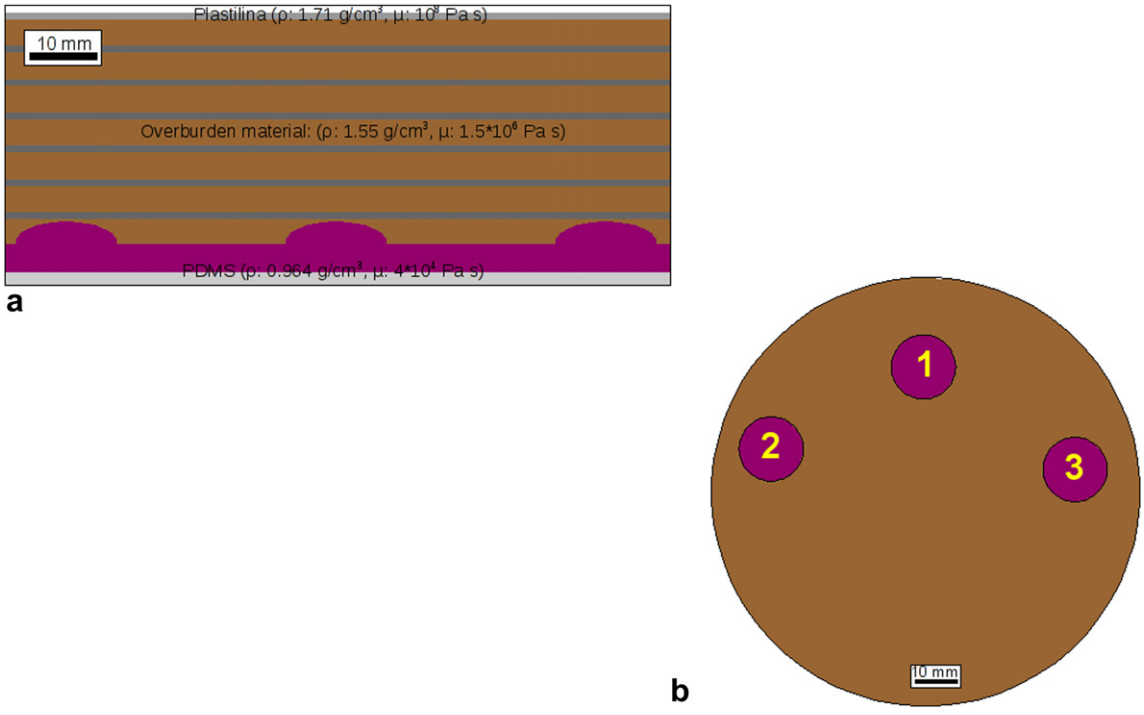

Fig. 4. Setup of the centrifuge experiment. Shown are both the buoyant PDMS layers – pure purple and impure grey – and its passively stratified overburden. On top of the purple PDMS layer three perturbations were installed to control the positions of the growing diapirs. For details of the applied material see Table 1 (For interpretation of the references to color in this figure legend, the reader is referred to the web version of this article.).

Table 1
Material properties of the experiment and its natural counterpart. Also listed are the scaling factors between model and nature.

	Model	Nature	Ratio model: nature
Overburden	Plasticine silicone mixture	Silicic rocks	
Density [kg/m]	1.55E + 03	2.70E + 03	5.74E – 01
Viscosity [Pa s]	2.00E + 06	1.00E + 22	2.00E – 16
Thickness [m]	3.40E – 02	3.40E + 03	1.00E – 05
Buoyant material	Pure PDMS	Felsic magma	
Density [kg/m^3]	9.64E + 02	1.68E + 03	5.74E – 01
Viscosity [Pa s]	2.40E + 04	1.00E + 20	2.40E – 16
Thickness [m]	4.00E – 03	4.00E + 02	1.00E – 05
	Impure PDMS	Mafic magma	
Density [kg/m]	1.17E + 03	2.05E + 03	5.71E – 01
Viscosity [Pa s]	5.00E + 05	2.08E + 21	2.40E – 16
Thickness [m]	4.00E – 03	4.00E + 02	1.00E – 05

(Fig. 5c and d). Around these two diapirs also rim synclines had developed (Fig. 5c and d). The internal structures of diapirs 2 and 3 differ strongly from that observed in diapir 1. The grey PDMS bodies within the balloon-shaped diapirs 2 and 3 do not copy the external geometry of the diapir, but form an upright, straight finger-shaped body from the PDMS source through the diapir stem and into their head (Fig. 5c and d). These "fingers" reach the top of the diapirs.

A compilation of the structural inventory of the model after centrifuging is displayed in Fig. 6.

3. Discussion

Our centrifuge model is a good example of how diapirs change their shape during their buoyancy-driven ascend, depending on (1) their position in relation to the level of neutral buoyancy of the buoyant material and (2) the viscosity of the material they are travelling through.

In our model, we are able to observe diapirs at two different stages of their evolution. While diapir 1 had reached its level of neutral buoyancy (i.e. extruded at the surface of the model), diapirs 2 and 3 were "frozen" at a deeper level, i.e. they were still rising when centrifuging stopped. The different evolutionary stages of these three diapirs are documented, in the first place, by their external geometry, i.e. by the purple PDMS bodies.

Diapir 1 is of a tabular shape, because it has reached the top of the model which acts as a boundary but at the same time as level of neutral buoyancy for the PDMS, since the overburden material is denser and the air above it is lighter than PDMS. Consequently, the diapir head had started to spread. The shape of this diapir does not any longer reflect the viscosity ratio m of ~0.01 (Table 2) between the buoyant material and its overburden. In contrast, the balloon-on-string geometry of diapirs 2 and 3 is the result of the high viscosity ratio m (Table 2).

The grey impure PDMS bodies inside the three diapirs differ in shape, too. The internal PDMS body within diapir 1 copies the tabular external shape of its purple precursor, but the grey buoyant bodies within diapirs 2 and 3 have a finger-like shape. Obviously, the grey buoyant body within diapir 1 had also reached its level of neutral buoyancy at the top of the model where it spread as the

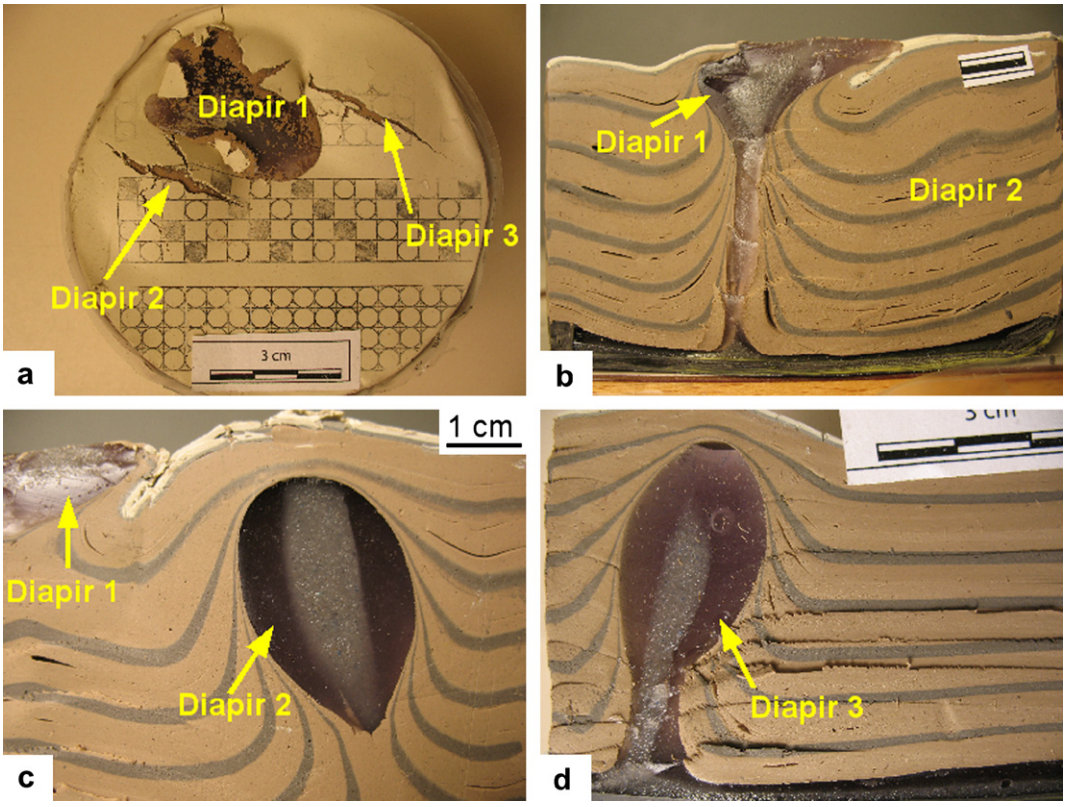

Fig. 5. a) Photograph of the model in map view after centrifuging. Three diapirs have risen leading to doming and fracturing of the overburden layers. Diapir 1 has even reached the surface and spread on top of the model. b) Section through the tabular diapir 1. The internal diapir copies the outline of the body. Rim synclines are developed in the ductile overburden, as well as isoclinal folds and even thrusts in the thin semibrittle plasticine layers on top of the model, where diapir 1 has extruded. c) Section through the balloon-on-string diapir 2. The internal, grey intrusive body has finger shape and does not at all follow the outline of the diapir. d) Section through diapir 3, which resembles diapir 2. Both these diapirs are framed by fully developed rim synclines.

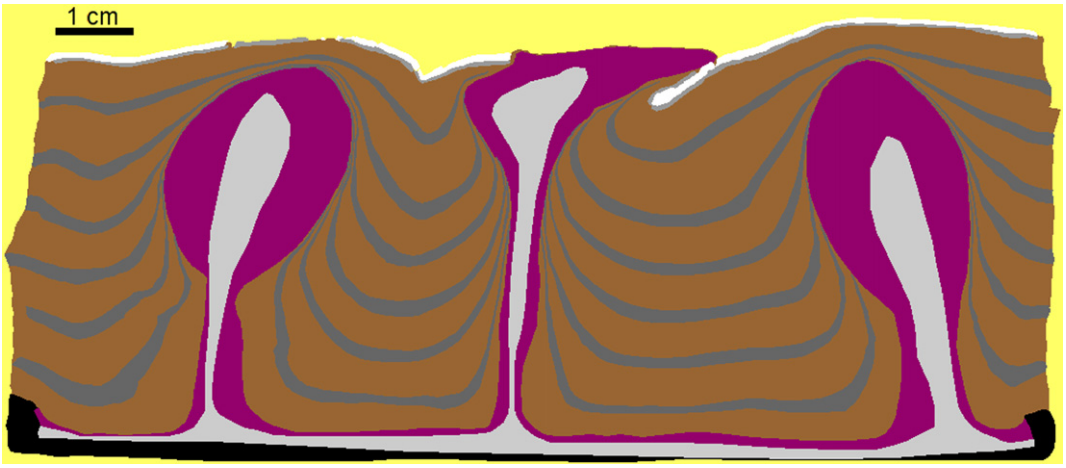

Fig. 6. Compilation of the resulting structures from the centrifuge experiment.

purple PDMS body did. Consequently, its shape follows the geometry of the purple diapir 1. In contrast, the grey, internal structures of diapirs 2 and 3 with their finger geometries do not at all copy the balloon-on-string shape of their purple precursors. Finger-shaped diapirs develop, according to Jackson and Talbot (1989), when a more viscous buoyant material rises through a less viscous medium. This is also the case in our experiment where m between the impure and the pure PDMS is ca. 20 (Table 2). Consequently, the impure grey PDMS with its higher viscosity (5×10^5 Pa s) behaves as a more viscous material rising through a less viscous pure PDMS (2.45×10^4 Pa s) which accommodates most of the deformation during the diapiric ascent of the grey PDMS.

Jackson and Talbot (1989) showed that even a passively stratified buoyant less viscous layer forms a finger-shaped internal structure within a balloon-on-string diapir. However, in their model, since all the diapiric materials have the same viscosity, with further rise of the diapir, the internal geometry of the ascending buoyant body develops a similar pattern as that of the external geometry. This is unlikely in the models which we report here, because the impure PDMS forming the "fingers" within the purple balloon-on-string diapirs 2 and 3 is more competent than the rest of the purple PDMS and does not accommodate as much deformation. As a result, the less viscous material accommodates most of the internal flow whereas the more viscous material maintains its finger-like geometry. Only when reaching the level of neutral buoyancy the grey impure PDMS starts to form a tabular body copying the shape of the surrounding purple diapiric structure.

The reason for the rise of the pure PDMS is, of course, buoyancy: it is much lighter than the ductile overburden. However, the impure PDMS is heavier than the pure PDMS and is probably entrained into the purple diapirs mainly due to the drag of the ascending pure buoyant material. Such entrainment of denser materials by diapirs have been reported and modeled by other researchers (Cruden et al., 1995; Koyi, 2000, 2001; Chemia et al., 2008). In our centrifuge model, we are not able to observe directly this entrainment, because this early stage of diapirism is not preserved within the model. Nevertheless, we can assume from the two preserved stages of diapirism (represented by diapir 1 – tabular – on one hand, and diapirs 2 and 3 – balloon-on-string – on the other hand) that the entrainment of the grey, impure PDMS into the rising purple, clean PDMS diapirs takes place very early during the ascent of the buoyant material. The finger shape of the impure, grey PDMS batches within the purple balloon-on-string diapirs 2 and 3, however, is then the result of internal flow of the less viscous clean, purple PDMS around the stiffer impure, grey PDMS during their rise.

Although we were not able to control the viscosity of our analogue materials by means of temperature changes, the finger-shaped grey PDMS bodies within diapirs 2 and 3 display the same rheological behaviour as a basalt dike intruding into a granitic magma chamber. As soon as a hot, low-viscous, possibly mafic magma enters the cooler, more viscous granitoid magma, it will be quenched, it will start to crystallize and its viscosity will increase dramatically. Consequently, the viscosity ratio between the entering and the hosting magma will turn over and will reach a similar or even higher value than the viscosity ratio between the impure and the clean PDMS of ca. 20. In case of mafic dikes intruding felsic magmas the viscosity reversal inhibits magma mixing and leads either to the preservation of the dikes or to mingling features such as enclave swarms. In case of our model, the relatively high viscosity ratio between the impure and the clean PDMS leads to the finger shape of the grey PDMS bodies within diapirs 2 and 3, which – geometrically – resemble (mafic) dikes within granitoid plutons. In case the hosting balloon-on-string diapirs would be elliptical in map view, the finger-shaped bodies would look like sheets giving them an even more dike-like appearance.

Mechanically, the finger-shaped grey PDMS bodies are not at all alike dikes which travel through the viscoelastic earth crust. They do not propagate due to the elastic response of the host material to the pressure built up at the dike tip, which in turn is the result of the buoyancy of the magma and the high fluid pressure within the conduit. Rather they start their upward movement passively as a result of drag and entrainment by the buoyantly rising clean, purple PDMS. However, a dike, which enters a pluton with partially molten and viscoplastic granitic magma does probably not either propagate by host rock cracking, even though it is driven by buoyancy and/or the magma pressure within the feeder conduit. Consequently, both, the grey impure PDMS fingers in the model and

Table 2
Viscosity ratios between the individual model materials.

No.	Model material	Viscosity [Pa s]		Viscosity ratio m
1	Plasticine silicone mixture	2.00E + 06	Between 2 and 1	1.20E − 02
2	Pure PDMS	2.40E + 04	Between 3 and 2	2.08E + 01
3	Impure PDMS	5.00E + 05		

dikes in nature, travel viscously through their host medium, either by entrainment or buoyancy + magma pressure.

Nevertheless, irrespective of the reasons for the rise and for the finger shape of the internal structures of diapirs 2 and 3, their formation next to a fully developed, tabular composite diapir is of interest. It shows that an intrusive body with a finger or sheet geometry within a balloon-shaped intrusion can develop into a tabular diapir-in-diapir structure when reaching its level of neutral buoyancy. Similarly, dikes and sheets within plutons may play a similar role in nested magma systems as the finger-shaped impure PDMS bodies within our experimentally derived diapirs 2 and 3 do: i.e. they may during the continued rise of the entire pluton develop into tabular bodies. Moreover, once established and stable (i.e. not disintegrated into enclave swarms) such fingers, sheets or "dikes" could act as conduits feeding – at a higher structural level – the individual magma batches of composite plutons. This is true, although the two examples for sheets within diapirs we have introduced – the Cannibal Creek and Chila plutons – differ clearly from our diapirs 2 and 3. The impure PDMS in diapirs 2 and 3 form single, large, straight fingers, while (1) the Chila Pluton contains numerous small dikes (Fig. 2a) and (2) the sheets in the Cannibal Creek are strongly curved (Fig. 2b). However, the processes that form and shape these structures in nature are much more complex than the processes in centrifuge experiments. A magma intruding an already established magma chamber may follow preexisting structures which can lead to the formation of numerous small dikes instead of one extended sheet. Magma chamber processes such as (diapiric) magma flow affect an intruded dike or sheet, bend it several times and even disrupt it to form enclave swarms (Fig. 1b).

4. Conclusions

The presented centrifuge experiment displays three diapirs which represent two different stages during the growth of a composite diapir: (1) diapirs 2 and 3 are fully developed, but still rising balloon-on-string diapirs; each includes a finger-shaped intrusive body; (2) diapir 1 has reached its level of neutral buoyancy; its tabular outline is copied by the internal, secondary intrusion. Diapirs 2 and 3 show that finger-shaped or sheet-like intrusions, which resemble intraplutonic dikes, can well be part of a nested magma system. These "dikes" occur as internal structures of *rising* composite diapirs, while *at their level of neutral buoyancy* composite diapirs have generally tabular shape – externally, as well as internally, as proven by our diapir 1 or several older centrifuge studies (Dietl and Koyi, 2002; Dietl et al., 2006). From our observations we can conclude that only during ascent the shape of a diapir does reflect the viscosity ratio between buoyant material and overburden. Moreover, our model is a good analogue for composite plutons which have reached different structural levels. Diapir 1 represents a typical concentrically expanded pluton or nested diapir (Paterson and Vernon, 1995) such as the Joshua Flat-Beer Creek Pluton and the Ardara Pluton. In contrast, diapirs 2 and 3 resemble circular plutons (in map view) which contain major sheets or extended systems of small dikes, such as the Cannibal Creek Pluton and Chila Pluton. Transferring the model situation to nature, this implies that these dikes or dike systems could be "nuclei" or feeder conduits for nested magma batches.

Acknowledgements

This research was funded by DFG project BA1443/16-1. Special thanks go to Martin van Kranendonk. Discussion with him brought the idea of this experiment up. Thanks for the very constructive review by Scott Paterson and also for the editorial work by Joao Hippertt. HAK is funded by the Swedish Research Council (VR).

References

Cruden, A., Koyi, H., Schmeling, H., 1995. Diapiric basal entrainment of mafic into felsic magma. Earth and Planetary Science Letters 131, 321–340.
Chemia, Z., Koyi, H.A., Schmeling, H., 2008. Modelling the rise and fall of exotic blocks in salt diapirs. Geophysical Journal International 172, 798–816.
Dietl, C., Koyi, H.A., 2002. Emplacement of nested diapirs: results of centrifuge modelling. Journal of the Virtual Explorer 6, 81–88.
Dietl, C., Koyi, H., de Wall, H., Gößmann, M., 2006. Centrifuge modelling of plutons intruding shear zones: application to the Fürstenstein Intrusive Complex (Bavarian Forest, Germany). Geodinamica Acta 19, 165–184.
Dietl, C., Longo, A., 2007. Thermal aureole around the Joshua Flat – Beer Creek Pluton, (California) requires multiple magma pulses: constraints from thermobarometry infra-red spectroscopy and numerical modelling. Geotectonic Research 95, 13–40.
Frost, T.P., Mahood, G.A., 1987. Field, chemical, and physical constraints on mafic felsic magma interaction in the Lamarck Granodiorite, Sierra Nevada, California. Geological Society of America Bulletin 99, 272–291.
Jackson, M.P.A., Talbot, C.J., 1989. Anatomy of mushroom shaped diapirs. Journal of Structural Geology 11, 211–230.
Jungmann, O., 2009. Platznahme von Chila- und Rama-Pluton (Nord-Äthiopien, Provinz Tigray): AMS-, thermobarometrische und geochemische Untersuchungen an zwei panafrikanischen Granitoiden. Unpublished diploma thesis, Goethe Universität Frankfurt am Main.
Koyi, H.A., 1991. Mushroom diapirs penetrating into high viscous overburden. Geology 19, 1229–1232.
Koyi, H.A., 2000. Analogue modelling of entrainment of non-evaporitic rocks by salt diapirs. In: Geertman, R.M. (Ed.), Proceedings of the 8th World Salt Symposium, vol. 1, pp. 149–153.
Koyi, H.A., 2001. Modelling the influence of sinking anhydrite blocks on salt diapirs targeted for hazardous waste disposal. Geology 29, 387–390.
Lister, J.R., Kerr, R.C., 1991. Fluid-mechanical models of crack propagation and their application to magma transport in dykes. Journal of Geophysical Research 96, 10049–10077.
Petford, N., Cruden, A.R., McCaffrey, K.J.W., Vigneresse, J.-L., 2000. Granite magma formation, transport and emplacement in the earth's crust. Nature 408, 669–673.
Paterson, S.R., Vernon, R.H., 1995. Bursting the bubble of ballooning plutons; a return to nested diapirs emplaced by multiple processes. Geological Society of America Bulletin 107, 1356–1380.
Sparks, R.S.J., Marshall, L., 1986. Thermal and mechanical constraints on mixing between mafic and silicic magmas. Journal of Volcanology and Geothermal Research 29, 99–124.
Spera, F.J., 1980. Aspects of magma transport. In: Hargraves, R.B. (Ed.), Physics of Magmatic Processes. Princeton University Press, Princeton, pp. 265–324.
Sigesmund, S., Becker, J.K., 2000. Emplacement of the Ardara Pluton (Ireland): new constraints from magnetic fabrics, rock fabrics and age dating. International Journal of Earth Sciences 89, 307–327.
Tadesse-Alemu, A., 1998. Geochemistry of neoproterozoic granitoids from the Axum area, northern Ethiopia. Journal of African Earth Sciences 27, 437–460.
Weijermars, R., 1986. Flow behaviour and physical chemistry of bouncing putties and related polymers in view of tectonic laboratory applications. Tectonophysics 124, 325–358.